Research Square

Preprints are preliminary reports that have not undergone peer review.
They should not be considered conclusive, used to inform clinical practice,
or referenced by the media as validated information.

The effect of light intensity on microalgae biofilm structures and physiology under continuous illumination

Yan GAO
Université Paris-Saclay, CentraleSupélec, LGPM
Olivier Bernard
Université Nice Côte d'Azur, Inria Sophia Antipolis Méditerranée, Biocore
Andrea Fanesi
Université Paris-Saclay, CentraleSupélec, LGPM
Patrick Perré
Université Paris-Saclay, CentraleSupélec, LGPM, CEBB
Filipa Lopes (filipa.lopes@centralesupelec.fr)
Université Paris-Saclay, CentraleSupélec, LGPM

Article

Keywords:

Posted Date: June 22nd, 2023

DOI: https://doi.org/10.21203/rs.3.rs-3058230/v1

License: This work is licensed under a Creative Commons Attribution 4.0 International License.
Read Full License

Additional Declarations: No competing interests reported.

Version of Record: A version of this preprint was published at Scientific Reports on January 11th, 2024.
See the published version at https://doi.org/10.1038/s41598-023-50432-6.

The effect of light intensity on microalgae biofilm structures and physiology under continuous illumination

Yan Gao[1,2], Olivier Bernard[2], Andrea Fanesi[1], Patrick Perré[3], and Filipa Lopes[1,*]

[1]Université Paris-Saclay, CentraleSupélec, LGPM, Gif-sur-Yvette, 91190, France
[2]Université Nice Côte d'Azur, Inria Sophia Antipolis Méditerranée, Biocore, Valbonne, 06902, France
[3]Université Paris-Saclay, CentraleSupélec, LGPM, CEBB, Pomacle, 51110, France
[*]filipa.lopes@centralesupelec.fr

ABSTRACT

Biofilm-based microalgae technology improves productivity, reduces energy consumption and facilitates harvesting. However, the effect of light received less attention than for planktonic cultures. This work assessed the effect of Photon Flux Density (PFD) on *Chlorella vulgaris* biofilm dynamics (structure, physiology, activity). Microalgae biofilms were cultivated in a flow-cell system with PFD from 100 to 500 $\mu\text{mol}\cdot\text{m}^{-2}\cdot\text{s}^{-1}$. In the first stage of biofilm development, uniform cell distribution was observed on the substratum exposed to 100 $\mu\text{mol}\cdot\text{m}^{-2}\cdot\text{s}^{-1}$ while cell clusters were formed under 500 $\mu\text{mol}\cdot\text{m}^{-2}\cdot\text{s}^{-1}$. Though similar specific growth rate in exponential phase (ca. 0.3 d^{-1}) was obtained under all light intensities, biofilm cells at 500 $\mu\text{mol}\cdot\text{m}^{-2}\cdot\text{s}^{-1}$ seem to be ultimately photoinhibited (lower final cell density). *Chlorella vulgaris* showed a remarkable capability to cope with high light. This was marked for sessile cells at 300 $\mu\text{mol}\cdot\text{m}^{-2}\cdot\text{s}^{-1}$, which reduce very rapidly (in two days) their chlorophyll-a content, most probably to reduce photodamage, while maintaining a high final cell density. Besides cellular physiological adjustments, our data demonstrate that cellular spatial organization is light-dependent.

Introduction

Microalgae are considered a promising resource for the production of food, feed, high-value biocompounds, and, in the long term, biofuels[1]. Currently, microalgae cultivation has been mainly carried out in suspension-based systems using either open systems (open ponds or raceways) or closed reactors (photobioreactors)[2,3]. Open ponds show advantages for microalgae cultivation compared to closed systems since they require less energy, their construction is easier and operational costs are reduced. They are the most widespread at industrial scales[3]. However, these suspension-based systems present a low biomass productivity due to inefficient light penetration, low CO_2 transfer rate, non-efficient mixing and non-sterile conditions. They also use large amounts of water and require large land area[3,4]. In suspended cultures, biomass is diluted, representing maximum 1% of the liquid mass so that harvesting is energy and cost demanding[4].

Biofilm-based systems have recently emerged and received more interest[5]. Their productivity is higher[4], and the costs of harvesting and dewatering are lower[6], mainly due to a lower energy demand[7]. Many photobioreactors with different configurations for microalgae biofilm cultivation have been proposed. Wang et al.[5] summarized some common designs of attached algal cultivation systems. Significant improvements of productivity in biofilm-based systems compared to suspended cultures have been reported[4,8,9] which could be due to the effective light penetration and CO_2 assimilation rate. For instance, Wang et al.[10] reported 100% effective illumination inside the *S. dimorphus* biofilms with biomass density of 107.6 $\text{g}\cdot\text{m}^{-2}$ under sunlight (1500-1600 $\mu\text{mol}\cdot\text{m}^{-2}\cdot\text{s}^{-1}$), while the effective illumination fraction was only 31.1% with the biomass density of 90 $\text{g}\cdot\text{m}^{-2}$ in a conventional open pond within the same light condition. Besides, a more efficient CO_2 transfer in biofilm than in suspension has been stated by Huang et al.[11] with biomass areal density improvement.

Algal biofilm-based systems are an emerging yet immature technology for which much remains to be understood[12]. Unlike planktonic cells that are suspended in the medium and subjected to mixing, microalgae biofilms are regarded as a slimy layer of microalgae that attach and grow on solid surfaces, presenting a 3D structure (spatial arrangement of the cells, polymers and voids) and with features strongly differing from their planktonic counterparts[13]. Biofilms are highly heterogeneous in time and space. They are characterized by high cell density, an extracellular polymer substances (EPS) matrix with physical, chemical, biological and metabolic heterogeneities[13] over depth. 3D structure has been shown to be strongly affected by environmental and operation factors such as shear stress[14], nutrients transport[15–17], and they are also species-dependent[18]. Moreover, the impact of environmental factors (light quality, quantity, nutrients, *etc*,) on biofilm growth, structure, cell physiology and regulation is largely unknown.

Light is a critical factor for microalgae growth. For planktonic cultures, the optimal Photon Flux Density (PFD) ranges from 100 to 400 $\mu mol \cdot m^{-2} \cdot s^{-1}$ in general, depending on the species[5,19–21]. Higher light intensities damage the photosynthetic apparatus. Interestingly, algae have the ability to photoacclimate to different light conditions in order to maximize the photosynthetic efficiency and reduce photodamage. Physiological changes are then triggered by the cell, such as the modification of photosystem size or chlorophyll content[22]. It is widely known that chlorophyll-a content decreases with intensified irradiance as a strategy of self-protection to cope with light stress. The dark adapted F_v/F_m derived from variable fluorescence measurements is an index of the health status of microalgal cells, indicating if there is light or nutrient stress on PSII[23–25]. Healthy microalgal cultures have F_v/F_m values in the range of 0.7 - 0.8[26], whereas a decrease in F_v/F_m suggests a decrease in PSII photochemistry efficiency or a disorder in or damage to the photosynthetic apparatus[27]. Algal cells can also adjust cellular composition in response to light changes, like carbon content, lipid content[28,29]. Other properties such as cell volume are also affected by light, and it has been shown that microalgae cell size is positively correlated to PFD[28,30,31].

However, unlike planktonic cultures, the impact of environmental factors (light quality, quantity, nutrients, *etc*,) on biofilm growth, structure, cell physiology and regulation is largely unknown. In this work, we assessed the dynamic of biofilm development under four light intensities, ranging from 100 to 500 $\mu mol \cdot m^{-2} \cdot s^{-1}$. 3D structure of biofilms, cell physiological adjustments (such as photoacclimation) and metabolic activity (photosynthesis and dark respiration) were measured. This is of paramount importance to better understand the overall functioning of photosynthetic populations developing in biofilm in order to further exploit them efficiently in bioproduction.

Results and Discussion

Physiological shift of microalgae cells from planktonic to sessile state

A sharp decrease in cell volume was observed for all light conditions during the first two days after inoculation, except for 500 $\mu mol \cdot m^{-2} \cdot s^{-1}$ which presents a significant increase (Figure 1A). The same trend was detected for the chlorophyll content and the maximum quantum yield (Figure 1B,C). This suggests a physiological acclimation of the cells when switching from planktonic to sessile state, potentially triggered by changes in the environmental conditions, as proposed by Li et al.,[32]. Indeed, even if the average PFD supplied to the two systems was similar, differences in light quantity and quality may have occurred from suspended to biofilm cultures. For example, in suspended cultures exposed to continuous light (inoculum), cells undergo fluctuating light due to auto-shading and agitation while they are submitted to constant PFD in biofilm state. This explains also the reduction of the F_v/F_m ratio after two days. At larger time scales (day 7 and day 15), cell volume and chlorophyll a content follow the day 2 trend as a function of PFD, but with a reduced difference. This could be explained by the light attenuation due to the film thickness. Other factors specific to biofilms, such as mechanical stress and/or quorum sensing as already reported for bacterial biofilms, should not though be excluded. It should be pointed out that this phenomenon has rarely been described in microalgae biofilms.

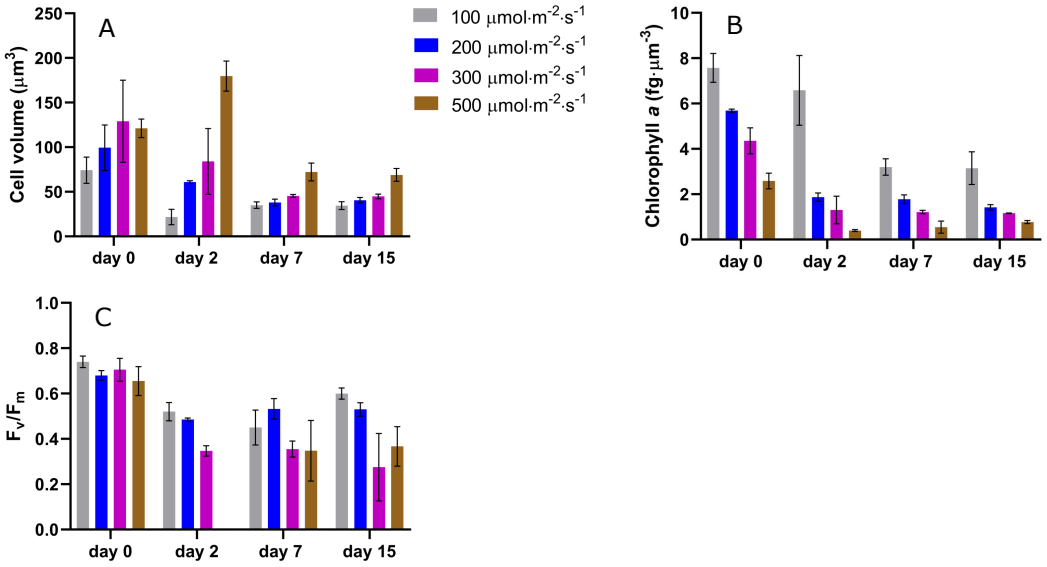

Figure 1. Evolution of biofilm cell physiological parameters over time. Data on Day 0 refers to the inoculum culture (A) cell volume; (B) chlorophyll-a content ($fg \cdot \mu m^{-3}$); (C) F_v/F_m dynamics.

Biofilm dynamics: biomass and physiological properties

The dynamics of light attenuation and cell density under 100, 200, 300 and 500 $\mu mol \cdot m^{-2} \cdot s^{-1}$ are shown in Figure 2. Both biomass indicators show biomass increase due to biofilm growth under all the light conditions. The highest light attenuation (ca. 30%) was obtained at day 15 in biofilms under 100 $\mu mol \cdot m^{-2} \cdot s^{-1}$ while those exposed to 200, 300 and 500 $\mu mol \cdot m^{-2} \cdot s^{-1}$ only attenuated 10% of the light. Interestingly, this marked difference in light attenuation is not due to a significant difference in cell density. Indeed, similar cell densities are observed at day 15 for biofilms exposed to light in the range of 100 to 300 $\mu mol \cdot m^{-2} \cdot s^{-1}$. Conversely, a significantly lower cell density is measured for 500 $\mu mol \cdot m^{-2} \cdot s^{-1}$ (Two-way ANOVA test, $p < 0.05$, n = 4), while light attenuation is not different from the one at 200 and 500 $\mu mol \cdot m^{-2} \cdot s^{-1}$. Light attenuation is indeed not only depending on cell density, but also on the cell chlorophyll content and on cell size.

PFD from 100 to 300 $\mu mol \cdot m^{-2} \cdot s^{-1}$ seems to be optimal for *Chlorella vulgaris* biofilm growth (Figure 2B). This range is in agreement with other studies described in the literature, reporting saturating rates in the range of 200 to 280 $\mu mol \cdot m^{-2} \cdot s^{-1}$ for *Chlorella* sp. biofilms[11,33,34]. Biofilms exposed to 100 $\mu mol \cdot m^{-2} \cdot s^{-1}$ show the highest light attenuation despite similar cell density and smaller cell volume. This indicates excellent light-gathering efficiency, evidenced by the high chlorophyll content compared with other conditions (Figure 1B). On the contrary, for the strong irradiance of 500 $\mu mol \cdot m^{-2} \cdot s^{-1}$, cell stress is induced, as shown on the low F_v/F_m ratio, and this eventually negatively impacts growth. The light stress is probably mitigated within the biofilm by the lower chlorophyll content, to harvest less photons, and by the attenuation rate which is surprisingly high when considering the lower pigment content and lower cell density compared to all the other conditions.

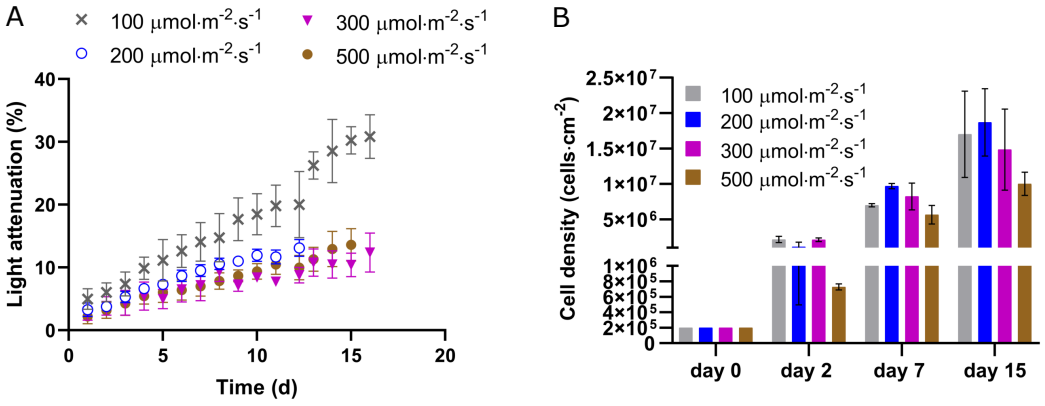

Figure 2. (A) Light attenuation dynamics; (B) Surface cell densities dynamics under 100, 200, 300, 500 $\mu mol \cdot m^{-2} \cdot s^{-1}$.

The dynamics of sessile cell volume and chlorophyll content are characterized by a general decreasing trend from day 2 to day 7. Afterwards, these values became stable, revealing full photoacclimation. Interestingly, a fast decrease in chlorophyll content, over only two days, occurred for light intensities higher than 100 $\mu mol \cdot m^{-2} \cdot s^{-1}$ while 7 days were required for 100 $\mu mol \cdot m^{-2} \cdot s^{-1}$. The time required to achieve photoacclimation seems thus to be light- and/or stress-dependent. The biofilms associated to higher level of stress (in terms of F_v/F_m) are those with a faster photoacclimation. Photoacclimation was also observed in *Scenedesmus dimorphus* and *Chlorella vulgaris* biofilms in 10 days period cultivation[10]. In another work, *Chlorella vulgaris* biofilms presented a decreased dry mass-based chlorophyll content on day 3 compared to day 1 when exposed to PFD conditions ranging from 40 to 280 $\mu mol \cdot m^{-2} \cdot s^{-1}$[11].

The stress level, as indicated by the F_v/F_m ratio, was different between planktonic and sessile cells. The measured range (0.66-0.74) suggests that suspended cultures (day 0) are non-stressed[35]. This ratio was lower than 0.6 for sessile cells, pointing out marked stress. Similarly, Wang et al.,[10] observed a much lower net photosynthesis rate in biofilms compared with suspended cultures exposed to the same PFD. Besides, F_v/F_m values reported in this study are slightly lower than those measured by Wang et al.[34]. Interestingly, after a first decline, the maximum quantum yield increased slightly from day 7 to day 15 for biofilms under 100 $\mu mol \cdot m^{-2} \cdot s^{-1}$. Our results are in agreement with the work of Lan et al.[36] who observed a decrease of F_v/F_m of *Microcoleus vaginatus* cells to (0.1-0.2) after inoculation, then recovering to 0.6 in 10 - 15 days[36]. This recovery pattern may reflect the progressive light reduction in the biofilm due to shading effects (Figure 2), associated with a decrease in chlorophyll content due to photoacclimation.

According to Figure 1C, biofilm cells seem to be more stressed under 300 and 500 $\mu mol \cdot m^{-2} \cdot s^{-1}$ (F_v/F_m mean values always under 0.4) than those at lower light intensity. In the absence of the fluctuating light achieved in suspension, these levels of lights are then able to trigger photo-stress. This is certainly accentuated further by the low biofilm development (only

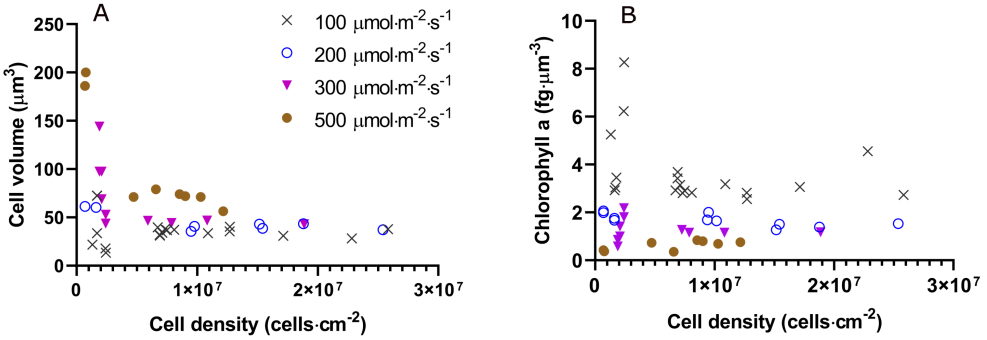

Figure 3. Cell volume (A), and chlorophyll-a content (B) changes with respect to cell density.

approximately 10% of the incident light was attenuated for the higher light intensities). Our observations are consistent with data from Wang et al.[34] who investigated the effect of light on the photosynthetic activity of a *Chlorella* sp. biofilm exposed to irradiances of 20, 50, 100, 200, and 400 μmol $\cdot$ m$^{-2}\cdot$s^{-1}. A F_v/F_m value higher than 0.65 with PFD of 100 μmol $\cdot$ m$^{-2}\cdot$s^{-1} was measured, but a significant decline was obtained when PFD reached 200 μmol $\cdot$ m$^{-2}\cdot$s^{-1} ($F_v/F_m < 0.6$) and 400 μmol $\cdot$ m$^{-2}\cdot$s^{-1} ($F_v/F_m = 0.45$), suggesting light stress[34].

Li et al.[33], measured a F_v/F_m value of 0.56 for biofilms of *Chlorella vulgaris* exposed to 500 μmol $\cdot$ m$^{-2}\cdot$s^{-1}. This higher value may be explained by differences in cell density and/or cultivation conditions (flow and light quality). Indeed, the inoculum cell density was much higher than that of our study (20 to 100 times). A stronger light attenuation might have then occurred, protecting cells from photoinhibition.

Effect of light intensity on biofilm growth, metabolism and physiology

Cell volume and chlorophyll content are plotted versus cell density in Figure 3. It appears that photoacclimated microalgae at similar cell density were significantly bigger at 500 μmol $\cdot$ m$^{-2}\cdot$s^{-1} compared to those at 100 μmol $\cdot$ m$^{-2}\cdot$s^{-1}. Cell volume was not significantly different for the lower light intensities. Few reports discuss light intensity effect on sessile cell size. Zhang et al.[37] observed that cell diameter remained at ca. 3.5 μm in a biofilm of *Chlorella vulgaris*, but in a limited range of PAR (50 to 104 μmol $\cdot$ m$^{-2}\cdot$s^{-1}). In agreement with our results, a positive correlation between cell volume and PFD has been described for suspended cultures[30,31,38]. In the work of Vejrazka et al.[38], the cell volume of *Chlamydomonas reinhardtii* doubled when cells were exposed to saturating light of 500 μmol $\cdot$ m$^{-2}\cdot$s^{-1} compared to that of 100 μmol $\cdot$ m$^{-2}\cdot$s^{-1}[38]. Accordingly, Winokur[30] showed a cell volume increase with light for eight *Chlorella* species. The increase of cell volume was reported for other species[31]: cell volume of *Skeletonema costatum* enlarged from 79 ± 10 μm^3 under 2.6 μmol $\cdot$ m$^{-2}\cdot$s^{-1} to 92 ± 7 μm^3 at 65 μmol $\cdot$ m$^{-2}\cdot$s^{-1} while for *D. tertiolecta* it increased from 69 ± 9 μm^3 under 2 μmol $\cdot$ m$^{-2}\cdot$s^{-1} to 112 ± 10 μm^3 at 200 μmol $\cdot$ m$^{-2}\cdot$s^{-1}. These observations can be explained by the overaccumulation of photosynthetic products (especially carbohydrates) at higher PFD[28]. It is worth remarking that a limit in cell volume was observed in these studies. It did not further increase for PFD higher than 130 μmol $\cdot$ m$^{-2}\cdot$s^{-1} and 400 μmol $\cdot$ m$^{-2}\cdot$s^{-1} for *S. costatum* and *D. tertiolecta*, respectively.

In line with the state of the art on photoacclimation[31,39] for suspended cultures, the highest chlorophyll-a content was observed under the lowest PFD of 100 μmol $\cdot$ m$^{-2}\cdot$s^{-1}. For light intensities of 200 and 300 μmol $\cdot$ m$^{-2}\cdot$s^{-1}, the content chlorophyll-a is much lower, about half with similar values, than at 100 μmol $\cdot$ m$^{-2}\cdot$s^{-1}. The same behavior has been reported for biofilms. Huang et al.,[11] saw a decreasing tendency of the biofilm chlorophyll content with PFD increasing from 40 to 200 μmol $\cdot$ m$^{-2}\cdot$s^{-1}. Remark that, since cells are bigger at higher light intensities, chlorophyll is more diluted in the cell.

Table 1. The maximum specific growth rate. The growth rate is expressed as the mean value $\pm$ standard deviation from total number of replicates of 21, 8, 10, 15 under light intensity of 100, 200, 300, 500 μmol $\cdot$ m$^{-2}\cdot$s^{-1}, respectively.

PFD μmol $\cdot$ m$^{-2}\cdot$s^{-1}	100	200	300	500
μ_l (d^{-1})	0.32 ±0.10	0.30 ±0.11	0.29 ±0.05	0.28 ±0.08
The average exponential phase	day 1-5	day 2-6	day 1-4	day 1-4

A mean growth rate of *ca*. 0.3 d^{-1} was measured for all the conditions tested (Table 1). Generally, biofilm grew exponentially around 4 to 5 days and linearly afterwards. Higher growth rates were though determined for *Chlorella* sp. biofilms in the literature: 0.45 d^{-1}[18] and 0.8 d^{-1}[14] in the work of Fanesi et al. , 0.4 - 0.5 d^{-1} (dependent on the light spectra) in the work of Yuan et al.,[40]. In another work, *Chlorella vulgaris* biofilm growth rate even reached 1.2 d^{-1}[41]. Many factors may explain these

differences. First, substratum properties (roughness, hydrophobicity, *etc.,*) are known to play an important role in cell adhesion[42]. Accordingly, a linear regression between the substratum roughness and biofilm productivity has been described elsewhere[43]. Unlike porous filtration membranes[40,41] used in some of these studies, a smooth glass surface was used here as biofilm support. Second, hydrodynamics conditions strongly affect biofilm development[18]. On the contrary of other works[18,40,41], a constant shear stress of 2.3 mPa was applied in our study, which may have contributed to a continuous cell detachment, therefore decreasing the growth rate. It has also been reported that the inoculum size influence biofilm growth[11,33]. Though similar shear stress and substratum material were used here and in the report of Fanesi et al.,[14], a lower initial biovolume was ued in the latter (ca. 25 times lower).

In biofilms with similar density, sessile cells exposed to high PFD (300 and 500 $\mu mol \cdot m^{-2} \cdot s^{-1}$) are clearly stressed. Different strategies are used by the cells to cope with excess of light and benefit growth, such as chlorophyll content reduction and/or storage compounds accumulation (carbohydrates, lipids). Interestingly, compared to biofilms grown at 100 $\mu mol \cdot m^{-2} \cdot s^{-1}$, those exposed to 300 $\mu mol \cdot m^{-2} \cdot s^{-1}$ presented higher metabolic activity (net photosynthetic and dark respiration rates were 4-fold (112 $\mu mol_{O_2} \cdot mg_{chl}^{-1} \cdot h^{-1}$) and 2-fold (72 $\mu mol_{O_2} \cdot mg_{chl}^{-1} \cdot h^{-1}$) higher compared to those at 100 (30 and 36 $\mu mol_{O_2} \cdot mg_{chl}^{-1} \cdot h^{-1}$, respectively) (see Supplementary Fig. S3 online). Their specific growth rates were similar despite a lower chlorophyll content. By reducing the pigment content and speeding up metabolic rates, cells were able to maintain the growth rate. On the other hand, the decline in chlorophyll content at 500 $\mu mol \cdot m^{-2} \cdot s^{-1}$ was not sufficient to counteract the excess of irradiance, so that photoinhibition occurred (a net photosynthetic rate of 63 $\mu mol_{O_2} \cdot mg_{chl}^{-1} \cdot h^{-1}$ was measured). Although cells succeeded in maintaining the growth rate in the early stages of biofilm development, a lower cell density was reported at the end of the assay. Additionally, cells increased in size, probably by accumulating storage compounds, to avoid severe photodamage and even cell death. Note that this increase in cell size partly compensates the lower growth rate in terms of total biomass production. Further experiments should be carried out to better understand this behavior. Parameters such as non-photochemical quenching (NPQ), photoprotectant pigments (mainly carotenoids) and intracellular compounds (lipids, carbohydrates) should be measured to go deeper in the understanding of photosynthetic mechanisms in biofilms at the transition towards photoinhibition.

Biofilm structure

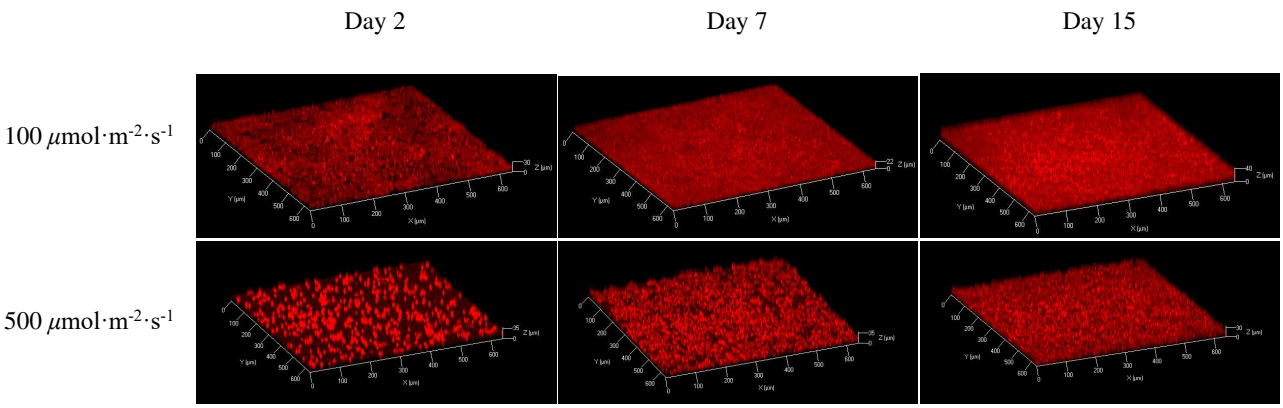

Figure 4. Confocal laser scanning microscopy (CLSM) observations of the 3D structure of biofilms under continuous light 100 $\mu mol \cdot m^{-2} \cdot s^{-1}$ and 500 $\mu mol \cdot m^{-2} \cdot s^{-1}$ at day 2, day 7, and day 15.

As a matter of illustration, the structural dynamics of biofilms formed at the lowest and the highest PFD (CLSM images and structural parameters) are shown in Figure 4 and Figure 5. Biovolume and average thickness increased over time in biofilms exposed to both light intensities (Figure 5A), in agreement with results of other studies at similar PFD[18]. This is also consistent with cell density dynamics shown in Figure 2B. Inhibition by intense light is also confirmed by CLSM analysis (two times lower biovolume at day 15 (t-test, $p<0.05$, $n = 4$)) despite similar maximum specific growth rates (0.30 ±0.06 d^{-1} and 0.28 ±0.05 d^{-1} under 100 and 500 $\mu mol \cdot m^{-2} \cdot s^{-1}$ respectively).

The maximum thickness shows though different patterns under the two irradiances. For 100 $\mu mol \cdot m^{-2} \cdot s^{-1}$, the maximum thickness was maintained stable at 27 μm during the initial four days and then increased gradually until the plateau at around 40 μm. By contrast, for 500 $\mu mol \cdot m^{-2} \cdot s^{-1}$, the maximum thickness rapidly increased from 27 μm to 37 μm surpassing the values observed at 100 $\mu mol \cdot m^{-2} \cdot s^{-1}$ in only three days, then kept approximately constant. These observations demonstrate that sessile cells' organization is light dependent. Since biofilms initiated from sparse cell density (ca. 15 μm distant from each other), the behavior under 100 $\mu mol \cdot m^{-2} \cdot s^{-1}$ implies that cells divided and dispersed evenly on the substratum but no clear

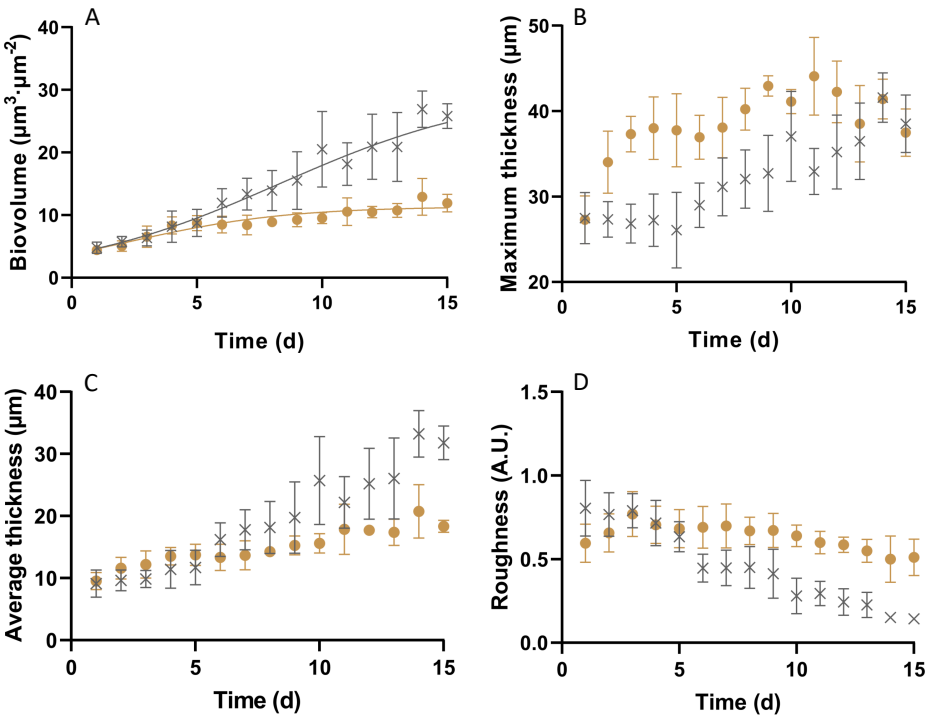

Figure 5. Dynamics of structural parameters derived from the z-stack acquired by Confocal Laser Scanning Microscopy (CLSM). (Biovolume, Maximum thickness, Average thickness, and Roughness) under continuous light of 100 μmol $\cdot$ m$^{-2}\cdot$s^{-1} (gray cross symbols) and 500 μmol $\cdot$ m$^{-2}\cdot$s^{-1} (brown solid dots), respectively.

growth occurs in depth in the early stage of biofilm formation. Afterwards, substratum was full covered and growth in depth happened. By contrast, cells exposed to 500 μmol $\cdot$ m$^{-2}\cdot$s^{-1} grow forming colonies as confirmed by the CLSM 3D structures (Figure 4). At the same time, they got bigger in only two days Figure 1A. The maximum thickness increased thus sharply during the early step (Figure 5B). Afterwards, voids between cell clusters were filled up through cell division and thickness kept roughly constant until the end of the assay. These results are in agreement with the roughness coefficient plotted in Figure 5D. Biofilms at 100 μmol $\cdot$ m$^{-2}\cdot$s^{-1} showed a decreasing trend, suggesting that they got smoother with time. Instead, in the latter stages of biofilm development, roughness at 500 μmol $\cdot$ m$^{-2}\cdot$s^{-1} is higher than at 100 μmol $\cdot$ m$^{-2}\cdot$s^{-1} (Figure 5D). From our findings, cell organization is likely to represent a mechanism of cellular adaptation to local conditions[16,37,44], and especially to PFD, in photosynthetic biofilms.

On the whole, we can hypothesize that physiological and structural adaptations occur when biofilm cells are exposed to high PFD. Indeed, stressed cells under 500 μmol $\cdot$ m$^{-2}\cdot$s^{-1} react very rapidly (2-3 days) to light by increasing their size (Figure 1A), decreasing the chlorophyll content (Figure 1B), dividing and organizing themselves in colonies instead of spreading on the substratum (Figure 4). They are thus able to perform exponential growth, dividing at the same rate as cells exposed to lower light (Table 1). Nevertheless, those physiological and structural adaptations, are not enough to maintain the growth rate. After a certain time, the growth rate decreases and a stationary plateau is reached where cell concentration is significantly lower compared to that at 100 μmol $\cdot$ m$^{-2}\cdot$s^{-1}. More experiments, combined with modelling approaches, are though required to fully understand this physiological and structural adaptation.

Material and Methods

Microalgae species and inoculum culture

Chlorella vulgaris SAG 211-11B (Göttingen, Germany) was cultivated in 3N-Bristol medium[45]. Inocula cultures were cultivated in a 100 mL glass tube with a working volume of 70 mL in a PSI MC1000 multicultivator (Photon systems instruments, Drásov, Czech Republic) at 25 $^{\circ}C$ with constant aeration by bubbling. Inocula cultures were photoacclimated for two weeks to the respective light regimes further applied to the biofilm studies (see subsection "Biofilm system set-up") and maintained in the exponential phase (cell concentration: 2 - 3 $\times 10^6$cells $\cdot$ mL^{-1}) by frequent dilutions (every 2-3 days).

Biofilm system set-up

C. vulgaris 211-11B biofilms were cultivated in a custom-made flow cell made of Poly-methyl methacrylate (PMMA) (40mm $\times$ 6mm $\times$ 3mm in length, width and height, respectively), with a cover glass as substratum, as presented in Figure 6. The set-up is already described by Le Norcy et al.[46] and Fanesi at al.[14]. Before inoculation, the system was first sterilized by sodium hypochlorite solution (0.5%, 0.1 mL $\cdot$ min^{-1}) for 3 h and then flushed with autoclaved distilled water. It was finally filled by 3N-Bristol medium overnight. To avoid bubbles development, the system was equilibrated with a flow rate of 0.1 mL $\cdot$ min^{-1} to throughout sterilization, washing and medium filling procedures. For inoculation, 3 mL pre-diluted inoculum culture with a cell concentration of 7×10^5cell $\cdot$ mL^{-1} was injected into each channel through an in-line luer injection port (Ibidi GmbH, Germany). After 24 h without medium flow to ensure cell attachment, fresh medium was added to the flow-cell system with laminar flow. With flow rate of 0.1 mL $\cdot$ min^{-1}, the shear stress (τ, mPa) can be estimated by equation (1) assuming the channel wide to be significantly larger than its height[47]:

$$\tau = \frac{6Q\mu}{wh^2} \tag{1}$$

where Q is the flow rate (μL $\cdot$ s^{-1}), μ is the dynamic viscosity of water (0.91 mPa $\cdot$ s^{-1}) at 24 °C, w and h are the width (mm) and height (mm) of the flow-cell channel, respectively.

Therefore, the dynamic flow parameters in this system were controlled at flow rate of 0.1 mL $\cdot$ min^{-1}, velocity of 0.093 mm $\cdot$ s^{-1}, Reynolds number of 0.37, and shear stress of 2.3 mPa. The temperature was controlled at 24 $\pm$ 1 °C.

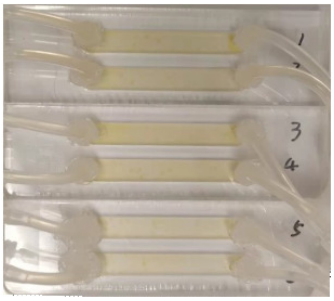

Figure 6. Custom-made flow-cell with *C. vulgaris* biofilms growing inside. Three flow-cells were placed side by side; Each of them has two separate channels.

Light was continuously supplied to the culture at 106 $\pm$ 2 μmol $\cdot$ m$^{-2}\cdot$s^{-1}, 200 $\pm$ 3 μmol $\cdot$ m$^{-2}\cdot$s^{-1}, 310 $\pm$ 3 μmol $\cdot$ m$^{-2}\cdot$s^{-1} and 496 $\pm$ 3 μmol $\cdot$ m$^{-2}\cdot$s^{-1}, respectively. They are denoted as 100, 200, 300, 500 μmol $\cdot$ m$^{-2}\cdot$s^{-1}, respectively. Light source is Light Emitting Diode (Alpheus LED, Montgeron, France) with light parameters controlled by the software Ether controller (v6.6.0.2) providing blue, red and white light. Light spectra information is provided in Supplementary data (400-500 nm: 30%, 500-600 nm: 21%, 600-700 nm: 48%, 700-800 nm: 1%). The PFD was measured by a Quantitherm PAR/Temp Sensor (Hansatech Instruments Ltd, Norfolk, The UK) which has uniform sensitivity to light spectra between 400 nm to 700 nm. The number of independent assays were 5, 4, 3, 4 for 100, 200, 300 and 500 μmol $\cdot$ m$^{-2}\cdot$s^{-1}, respectively. For each independent assay, we ran 6 channels as replicates.

Physiological parameters

Sessile cell physiology: cell volume, chlorophyll-a content, the maximum quantum yield of PSII-F_v/F_m, were assessed by off-line measurements on day 2, day 7, and day 15, respectively, by extracting the cells from each channel. Physiology of the inoculum culture (day 0) was analyzed to compare with that of biofilm cells.

Cell volume

Cell volume was measured by image acquisition through microscope imaging (Brigthfield in transmission mode) and subsequent image analysis (software ImageJ v1.48). On day 2, the low cell density was suitable for direct observation and the cell volume was measured in *situ*. For longer times, the cells were withdrawn, concentrated (to $1\times10^8 - 2\times10^8$cells $\cdot$ mL^{-1} by centrifugation at 14.5 krpm) and observed by optical microscopy on days 7 and day 15. 2D images were first obtained by the inverted Zeiss LSM 700 Confocal Laser Scanning Microscope (CLSM, Carl Zeiss microscopy GmbH, Jena, Germany) with Zen 10.0 software black edition (Carl Zeiss microscopy GmbH, Jena, Germany). LD Plan-Neofluar 20 $\times$ 0.4 Korr M27 objective with a 0.4 N.A. was used to take the picture with a frame size of 256 $\times$ 256 pixels (pixel size: 0.32 μm) and image size of 82.2 $\times$ 82.2 μm^2. On the other hand, optical track channel (TV1) was used for optical microscopy acquisition. The 2D

image including cells were analysed by ImageJ v1.48 software directly. The image type set to 8-bit before thresholding. After making binary of the image and all cells being filled in black with a white background, the area of each cell was estimated. The cell size limit was set as 0- infinity with the pixel units concerned. Assuming all cells to be spheres of similar diameter, the cell volume can be determined from the cell area (equation (2)):

$$Cell\ volume = \frac{4}{3} \cdot A \cdot \sqrt{\frac{A}{\pi}} \tag{2}$$

where A is the area of the microalgae cell in the 2D-image.

Chlorophyll-a content

Chlorophyll-a was extracted in DMSO (Dimethyl-sulphoxide) according to (Wellburn 1994)[48]. First, cells (range: $4 \times 10^6 - 10 \times 10^6$ cells) were filtrated on glass fiber filters (Fisher Scientific, size: 47 mm, EU). The filter was cut into 5 mm strip and then submerged in 1 mL DMSO. Chlorophyll-a extraction was carried out for 40 min at room temperature in the dark. After being centrifuged for 5 min with 1300 rpm, the supernatant was transferred to a 1.5 mL cuvette for absorbance measurement by a UV Visible Spectrophotometer (Thermo Fisher Scientific, EVOLUTION 60s, China). Chlorophyll-a ($\mu g \cdot mL^{-1}$) was calculated with equation (3):

$$Chlorophyll - a = 12.19 \cdot abs665 - 3.45 \cdot abs649 \tag{3}$$

Where abs665 and abs649 refer to the absorption at wavelength 665 nm and 649 nm, respectively. Chlorophyll-a content per cell volume ($fg \cdot \mu m^{-3}$) was then calculated.

Maximum quantum yield of PSII

The maximum quantum yield of PSII (F_v/F_m) of re-suspended biofilm cells was measured by a portable pulse amplitude modulation (PAM) fluorometer (AquaPen, Photon Systems Instruments, AP110C, Czech Republic, software FluorPen v1.0.1.8). According to the chlorophyll-a content, the cell concentration was adjusted to the range of 5×10^5 - 1×10^6 cells $\cdot mL^{-1}$ with medium in a 4 mL cuvette with 3 mL working volume and exposed to darkness for 15 min before measurement. The wavelengths used were 455 nm for fluorescence excitation and 667 nm -750 nm for fluorescence detection. The F_v/F_m which represents the maximum quantum yield or maximum photosynthetic potential of PSII was calulated with equation (4):

$$F_v/F_m = (F_m - F_0)/F_m \tag{4}$$

where F_0 is the minimum fluorescence yield determined after dark adaptation; F_m is the maximal fluorescence measured after excitation by a 0.8 s saturation light pulse with intensity of 3000 $\mu mol \cdot m^{-2} \cdot s^{-1}$. F_v is the difference between F_m and F_0.

3D structure of biofilms

Biofilm development under different light conditions was monitored in *situ* and non-destructively by an inverted Zeiss LSM 700 Confocal Laser Scanning Microscope (CLSM, Carl Zeissmicroscopy GmbH, Jena, Germany). Microalgae biofilm were imaged using CLSM through Z-stack controlled by the Zen 10.0 software black edition (Carl Zeiss microscopy GmbH, Jena, Germany). All biofilm 3D structures were acquired through a LD Plan-Neofluar 20x0.4 Korr M27 objective with a 0.4 N.A. (numerical aperture). Each slice has a frame size of 512 × 512 pixels and image size of 638.9 × 638.9 μm^2. Pixel size is 1.25 μm. Each z-step is 3.94 μm. One laser channel was applied to detect microalgal chlorophyll-a autofluorescence which was excited by 5-mW solid-state diode laser at 639 nm and detected at 615 nm after the long pass (CP) filter. For continuous light 100 $\mu mol \cdot m^{-2} \cdot s^{-1}$, the laser power was set at 1.0 and the gain (master) of the channel was set at 650. For continuous light at 500 $\mu mol \cdot m^{-2} \cdot s^{-1}$, chlorophyll content was too low to be detected with the setting used for 100 $\mu mol \cdot m^{-2} \cdot s^{-1}$. Therefore, the laser power was increased to 5.5 and the gain (master) was set at 680.

Biofilm of each flow-cell channel was measured in *situ* at five positions along the channel to obtain an average index of the biofilm structure. Measurements were carried out every 24 h to follow the biofilm structural dynamics. Biofilm architecture was characterized by the following parameters: biovolume ($\mu m^3 \cdot \mu m^{-2}$), maximum thickness (μm), average thickness (μm), roughness coefficient (A.U.) (ImageJ 1.48v software[49], plug-in COMSTAT 2.1 from Technical University of Denmark[50]). It is worth noting that autofluorescence of cells is related to chlorophyll within chloroplast. However, to be in accordance with the terminology presented in most of the literature, we consider the increase of autofluorescence as cells proliferation, though autofluorescence does not quantify the cells.

Biomass

Cell density

Biofilm cells were harvested from each channel by flushing Bristol medium through it, at least twice. Cell concentration was kept in the range of 1×10^4 to 6×10^5 cells $\cdot$ mL^{-1} by medium dilution and then measured by Guava easyCyte 5 flow cytometer (Millipore corporation 25801 Industrial Blvd Hayward, CA94545) with chlorophyll-a excitation at 488 nm and fluorescence detection at 680 nm . Aerial cell density was obtained from total cell number in one channel divided by the surface of the substratum of the channel (0.24 cm^2).

Light transmittance

Light transmission through the biofilm was calculated daily based on the difference between PFD above and below the flow-cell (equation (5)) measured by the light meter (LI-190/R; LI-COR Biosciences GmbH).

$$Light\ attenuation = \frac{I_{in} - I_{out}}{I_{in}} \times 100\% \tag{5}$$

where I_{in} refers to incident light on the top of the flow-cell, I_{out} refers to output light through the channel with biofilm (mean of three positions' outputs along the channel).

Growth rate

Biofilm specific growth rate was determined using light transmittance data.

The light transmittance in biofilms follows the Lambert-Beer Law:

$$I_{out} = I_{in} e^{-k \cdot X},$$

where X is the biomass, k is the light extinction coefficient. Thus:

$$X = \frac{1}{k} ln \frac{I_{in}}{I_{out}}.$$

Accordingly, the specific growth rate μ_l based on light transmittence is the slope of the regression between $ln(ln\frac{I_{in}}{I_{out}})$ and time t. At least four data points are used for the determination of the specific growth rate.

Statistics

Results are presented as mean and standard deviation. One-way and two-way ANOVA were proceeded by GraphPad prism 8.0 to test the statistical significance difference of means between different light regimes and time points. The level of significance was set at 0.05.

Conclusions

In this study, we clearly demonstrated that *Chlorella vulgaris* biofilm 3D structure, physiology (cell size, chlorophyll content) are affected by light intensity. Our data confirm that sessile cells react to light intensity by adjusting the chlorophyll content (a decrease in chlorophyll per volume unit is observed with increased light) as in suspended cultures. In addition, for the first time, a regulation mechanism through cell organization and growth is highlighted in photosynthetic biofilms to cope with excess of light. Changes in physiology and photosynthetic activity were also reported when cells switch from suspended to sessile state, suggesting cell acclimation to the new lifestyle. Light conditions that maximize cell density of *Chlorella vulgaris* biofilms were identified (range between 100 and 300 μmol $\cdot$ m$^{-2}\cdot$s^{-1}). On the whole, this study gave some new insights into physiological and structural mechanisms occurring in photosynthetic biofilms which are required for biofilm-based system's operation and optimization.

Data availability

The datasets generated and/or analyzed during the current study are not publicly available but are available from the corresponding author on a reasonable request.

References

1. Bhattacharya, M. & Goswami, S. Microalgae–a green multi-product biorefinery for future industrial prospects. Biocatal. Agric. Biotechnol. **25**, 101580 (2020).
2. Borowitzka, M. A. Commercial production of microalgae: ponds, tanks, tubes and fermenters. J. biotechnology **70**, 313–321 (1999).
3. Costa, J. A. V., Freitas, B. C. B., Santos, T. D., Mitchell, B. G. & Morais, M. G. Open pond systems for microalgal culture. In Biofuels from Algae, 199–223 (Elsevier, 2019).
4. Gross, M. & Wen, Z. Yearlong evaluation of performance and durability of a pilot-scale revolving algal biofilm (rab) cultivation system. Bioresour. technology **171**, 50–58 (2014).
5. Wang, J., Liu, W. & Liu, T. Biofilm based attached cultivation technology for microalgal biorefineries—a review. Bioresour. technology **244**, 1245–1253 (2017).
6. Christenson, L. B. & Sims, R. C. Rotating algal biofilm reactor and spool harvester for wastewater treatment with biofuels by-products. Biotechnol. bioengineering **109**, 1674–1684 (2012).
7. Yang, J. et al. Life-cycle analysis on biodiesel production from microalgae: water footprint and nutrients balance. Bioresour. technology **102**, 159–165 (2011).
8. Gross, M., Mascarenhas, V. & Wen, Z. Evaluating algal growth performance and water use efficiency of pilot-scale revolving algal biofilm (rab) culture systems. Biotechnol. Bioeng. **112**, 2040–2050 (2015).
9. Choudhary, P., Malik, A. & Pant, K. K. Mass-scale algal biomass production using algal biofilm reactor and conversion to energy and chemical precursors by hydropyrolysis. ACS Sustain. Chem. & Eng. **5**, 4234–4242 (2017).
10. Wang, J., Liu, J. & Liu, T. The difference in effective light penetration may explain the superiority in photosynthetic efficiency of attached cultivation over the conventional open pond for microalgae. Biotechnol. for biofuels **8**, 1–12 (2015).
11. Huang, Y. et al. Comparison of chlorella vulgaris biomass productivity cultivated in biofilm and suspension from the aspect of light transmission and microalgae affinity to carbon dioxide. Bioresour. technology **222**, 367–373 (2016).
12. Gross, M., Jarboe, D. & Wen, Z. Biofilm-based algal cultivation systems. Appl. microbiology biotechnology **99**, 5781–5789 (2015).
13. De Beer, D. & Stoodley, P. Microbial biofilms. Prokaryotes **1**, 904–937 (2006).
14. Fanesi, A. et al. Shear stress affects the architecture and cohesion of chlorella vulgaris biofilms. Sci. Reports **11**, 1–11 (2021).
15. De Beer, D., Stoodley, P., Roe, F. & Lewandowski, Z. Effects of biofilm structures on oxygen distribution and mass transport. Biotechnol. bioengineering **43**, 1131–1138 (1994).
16. Yuan, H. et al. Analyzing microalgal biofilm structures formed under different light conditions by evaluating cell–cell interactions. J. Colloid Interface Sci. **583**, 563–570 (2021).
17. de Beer, D., Stoodley, P. & Lewandowski, Z. Measurement of local diffusion coefficients in biofilms by microinjection and confocal microscopy. Biotechnol. bioengineering **53**, 151–158 (1997).
18. Fanesi, A., Paule, A., Bernard, O., Briandet, R. & Lopes, F. The architecture of monospecific microalgae biofilms. Microorganisms **7**, 352 (2019).
19. Yeh, K.-L., Chang, J.-S. & chen, W.-m. Effect of light supply and carbon source on cell growth and cellular composition of a newly isolated microalga chlorella vulgaris esp-31. Eng. Life Sci. **10**, 201–208 (2010).
20. Khan, M. I., Shin, J. H. & Kim, J. D. The promising future of microalgae: current status, challenges, and optimization of a sustainable and renewable industry for biofuels, feed, and other products. Microb. cell factories **17**, 1–21 (2018).
21. Mantzorou, A. & Ververidis, F. Microalgal biofilms: A further step over current microalgal cultivation techniques. Sci. Total. Environ. **651**, 3187–3201 (2019).
22. Raps, S., Wyman, K., Siegelman, H. W. & Falkowski, P. G. Adaptation of the cyanobacterium microcystis aeruginosa to light intensity. Plant Physiol. **72**, 829–832 (1983).
23. Maxwell, K. & Johnson, G. N. Chlorophyll fluorescence—a practical guide. J. experimental botany **51**, 659–668 (2000).
24. Masojidek, J., Koblizek, M. & Torzillo, G. Photosynthesis in microalgae. Handb. microalgal culture: biotechnology applied phycology 20 (2004).

25. Qi, H., Wang, J. & Wang, Z. A comparative study of maximal quantum yield of photosystem ii to determine nitrogen and phosphorus limitation on two marine algae. J. sea research **80**, 1–11 (2013).

26. Richmond, A. & Hu, Q. Handbook of microalgal culture: applied phycology and biotechnology (John Wiley & Sons, 2013).

27. Lichtenthaler, H., Buschmann, C. & Knapp, M. How to correctly determine the different chlorophyll fluorescence parameters and the chlorophyll fluorescence decrease ratio rfd of leaves with the pam fluorometer. Photosynthetica **43**, 379–393 (2005).

28. Claustre, H. & Gostan, J. Adaptation of biochemical composition and cell size to irradiance in two microalgae: Possible ecological implications. Mar. ecology progress series. Oldendorf **40**, 167–174 (1987).

29. Lima, S. et al. Flashing light emitting diodes (leds) induce proteins, polyunsaturated fatty acids and pigments in three microalgae. J. Biotechnol. **325**, 15–24 (2021).

30. Winokur, M. Growth relationships of chlorella species. Am. J. Bot. 118–129 (1948).

31. Falkowski, P. G. & Owens, T. G. Light—shade adaptation 1: Two strategies in marine phytoplankton. Plant Physiol. **66**, 592–595 (1980).

32. Li, S. Effect of process operational factors on Chlorella vulgaris biofilms : from cell mechanisms to process optimization. Theses, Université Paris-Saclay (2022).

33. Li, S. F., Fanesi, A., Martin, T. & Lopes, F. Biomass production and physiology of chlorella vulgaris during the early stages of immobilized state are affected by light intensity and inoculum cell density. Algal Res. **59**, 102453 (2021).

34. Wang, Y. et al. The self-adaption capability of microalgal biofilm under different light intensities: Photosynthetic parameters and biofilm microstructures. Algal Res. **58**, 102383 (2021).

35. Malapascua, J. R., Jerez, C. G., Sergejevová, M., Figueroa, F. L. & Masojídek, J. Photosynthesis monitoring to optimize growth of microalgal mass cultures: application of chlorophyll fluorescence techniques. Aquatic biology **22**, 123–140 (2014).

36. Lan, S., Wu, L., Yang, H., Zhang, D. & Hu, C. A new biofilm based microalgal cultivation approach on shifting sand surface for desert cyanobacterium microcoleus vaginatus. Bioresour. Technol. **238**, 602–608 (2017).

37. Zhang, J. & Perré, P. Gas production reveals the metabolism of immobilized chlorella vulgaris during different trophic modes. Bioresour. Technol. **315**, 123842 (2020).

38. Vejrazka, C., Janssen, M., Streefland, M. & Wijffels, R. H. Photosynthetic efficiency of chlamydomonas reinhardtii in flashing light. Biotechnol. bioengineering **108**, 2905–2913 (2011).

39. Lehmuskero, A., Chauton, M. S. & Boström, T. Light and photosynthetic microalgae: A review of cellular-and molecular-scale optical processes. Prog. oceanography **168**, 43–56 (2018).

40. Yuan, H. et al. Effect of light spectra on microalgal biofilm: Cell growth, photosynthetic property, and main organic composition. Renew. Energy **157**, 83–89 (2020).

41. Ye, Y. et al. Optimizing culture conditions for heterotrophic-assisted photoautotrophic biofilm growth of chlorella vulgaris to simultaneously improve microalgae biomass and lipid productivity. Bioresour. Technol. **270**, 80–87 (2018).

42. Hu, Y., Xiao, Y., Liao, K., Leng, Y. & Lu, Q. Development of microalgal biofilm for wastewater remediation: from mechanism to practical application. J. Chem. Technol. & Biotechnol. **96**, 2993–3008 (2021).

43. Zhang, Q. et al. Cultivation of algal biofilm using different lignocellulosic materials as carriers. Biotechnol. for biofuels **10**, 1–16 (2017).

44. Zhang, X. et al. Cell surface energy affects the structure of microalgal biofilm. Langmuir **36**, 3057–3063 (2020).

45. Levasseur, W., Taidi, B., Lacombe, R., Perre, P. & Pozzobon, V. Impact of seconds to minutes photoperiods on chlorella vulgaris growth rate and chlorophyll a and b content. Algal research **36**, 10–16 (2018).

46. Le Norcy, T. et al. A new method for evaluation of antifouling activity of molecules against microalgal biofilms using confocal laser scanning microscopy-microfluidic flow-cells. Int. Biodeterior. & Biodegrad. **139**, 54–61 (2019).

47. Hart, J. W., Waigh, T. A., Lu, J. R. & Roberts, I. S. Microrheology and spatial heterogeneity of staphylococcus aureus biofilms modulated by hydrodynamic shear and biofilm-degrading enzymes. Langmuir **35**, 3553–3561 (2019).

48. Wellburn, A. R. The spectral determination of chlorophylls a and b, as well as total carotenoids, using various solvents with spectrophotometers of different resolution. J. plant physiology **144**, 307–313 (1994).

49. Schneider, C. A., Rasband, W. S. & Eliceiri, K. W. Nih image to imagej: 25 years of image analysis. Nat. methods **9**, 671–675 (2012).

50. Heydorn, A. et al. Quantification of biofilm structures by the novel computer program comstat. Microbiology **146**, 2395–2407 (2000).

Acknowledgements

This research was financially supported by the China Scholarship Council and ANR PhotoBiofilm Explorer/LaSIPS Greenbelt.

Author contributions

Y.G, F.L and A.F conceived the experiment. F.L and A.F contributed to the supervision of the experiments. Y.G, F.L, A.F, P.P and O.B analysed the results. Y.G wrote the first manuscript version which was updated by all the authors.

Additional information

We declare no conflict of interest.

Supplementary Files

This is a list of supplementary files associated with this preprint. Click to download.

- Supplementarydata.pdf